

GEOPHYSICAL MONOGRAPH SERIES

**AGU**  
ADVANCING EARTH  
AND SPACE SCIENCE

# Global Drought and Flood

Observation, Modeling, and  
Prediction

*Editors*

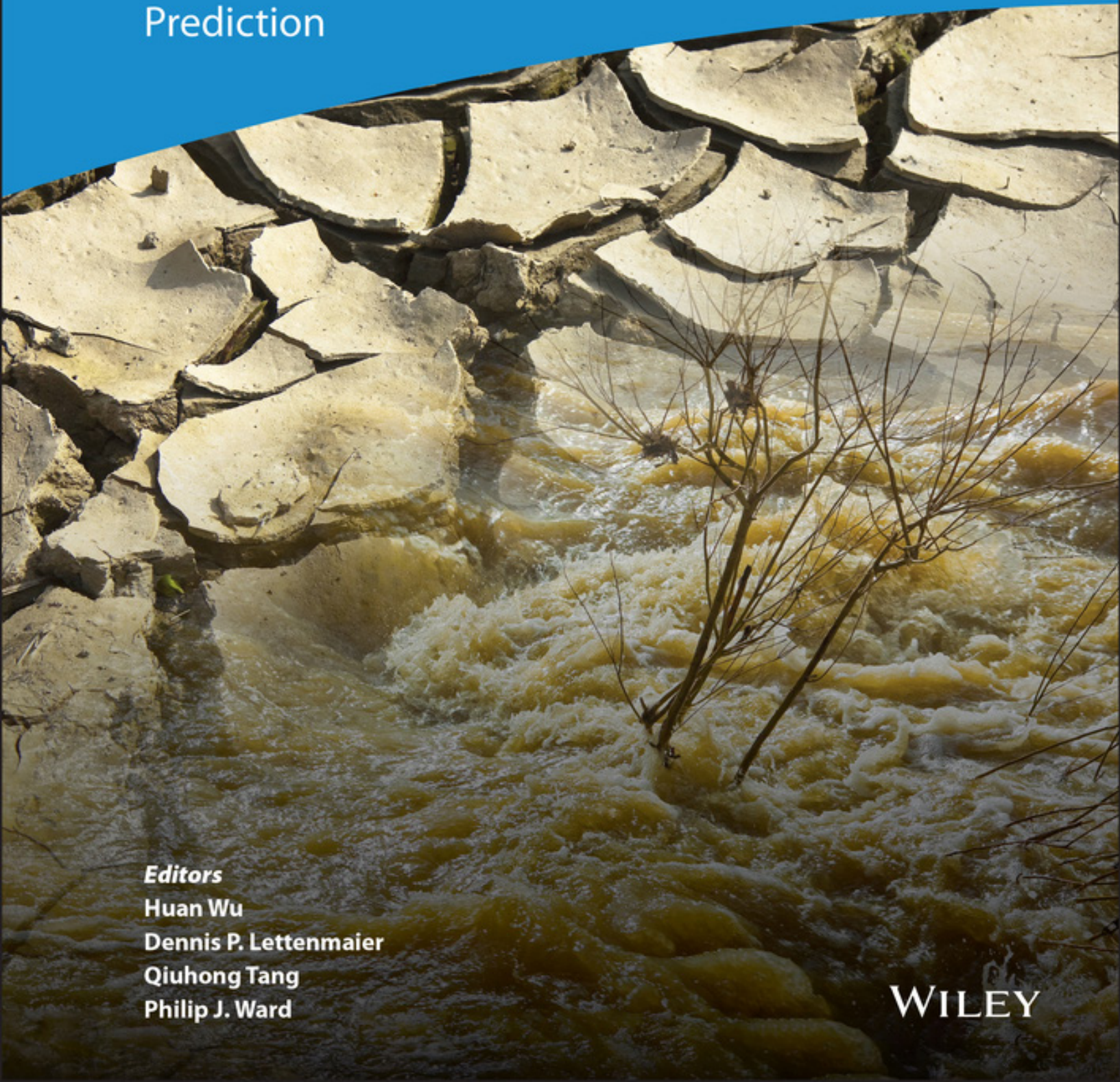
Huan Wu

Dennis P. Lettenmaier

QiuHong Tang

Philip J. Ward

**WILEY**





---

Geophysical Monograph Series

## Geophysical Monograph Series

- 214 **Extreme Events: Observations, Modeling and Economics** Mario Chavez, Michael Ghil, and Jaime Urrutia-Fucugauchi (Eds.)
- 215 **Auroral Dynamics and Space Weather** Yongliang Zhang and Larry Paxton (Eds.)
- 216 **Low-Frequency Waves in Space Plasmas** Andreas Keiling, Dong-Hun Lee, and Valery Nakariakov (Eds.)
- 217 **Deep Earth: Physics and Chemistry of the Lower Mantle and Core** Hidenori Terasaki and Rebecca A. Fischer (Eds.)
- 218 **Integrated Imaging of the Earth: Theory and Applications** Max Moorkamp, Peter G. Lelievre, Niklas Linde, and Amir Khan (Eds.)
- 219 **Plate Boundaries and Natural Hazards** Joao Duarte and Wouter Schellart (Eds.)
- 220 **Ionospheric Space Weather: Longitude and Hemispheric Dependences and Lower Atmosphere Forcing** Timothy Fuller-Rowell, Endawoke Yizengaw, Patricia H. Doherty, and Sunanda Basu (Eds.)
- 221 **Terrestrial Water Cycle and Climate Change Natural and Human-Induced Impacts** Qihong Tang and Taikan Oki (Eds.)
- 222 **Magnetosphere-Ionosphere Coupling in the Solar System** Charles R. Chappell, Robert W. Schunk, Peter M. Banks, James L. Burch, and Richard M. Thorne (Eds.)
- 223 **Natural Hazard Uncertainty Assessment: Modeling and Decision Support** Karin Riley, Peter Webley, and Matthew Thompson (Eds.)
- 224 **Hydrodynamics of Time-Periodic Groundwater Flow: Diffusion Waves in Porous Media** Joe S. Depner and Todd C. Rasmussen (Auth.)
- 225 **Active Global Seismology** Ibrahim Cemen and Yucel Yilmaz (Eds.)
- 226 **Climate Extremes** Simon Wang (Ed.)
- 227 **Fault Zone Dynamic Processes** Marion Thomas (Ed.)
- 228 **Flood Damage Survey and Assessment: New Insights from Research and Practice** Daniela Molinari, Scira Menoni, and Francesco Ballio (Eds.)
- 229 **Water-Energy-Food Nexus – Principles and Practices** P. Abdul Salam, Sangam Shrestha, Vishnu Prasad Pandey, and Anil K Anal (Eds.)
- 230 **Dawn–Dusk Asymmetries in Planetary Plasma Environments** Stein Haaland, Andrei Rounov, and Colin Forsyth (Eds.)
- 231 **Bioenergy and Land Use Change** Zhangcai Qin, Umakant Mishra, and Astley Hastings (Eds.)
- 232 **Microstructural Geochronology: Planetary Records Down to Atom Scale** Desmond Moser, Fernando Corfu, James Darling, Steven Reddy, and Kimberly Tait (Eds.)
- 233 **Global Flood Hazard: Applications in Modeling, Mapping and Forecasting** Guy Schumann, Paul D. Bates, Giuseppe T. Aronica, and Heiko Apel (Eds.)
- 234 **Pre-Earthquake Processes: A Multidisciplinary Approach to Earthquake Prediction Studies** Dimitar Ouzounov, Sergey Pulinet, Katsumi Hattori, and Patrick Taylor (Eds.)
- 235 **Electric Currents in Geospace and Beyond** Andreas Keiling, Octav Marghitu, and Michael Wheatland (Eds.)
- 236 **Quantifying Uncertainty in Subsurface Systems** Celine Scheidt, Lewis Li, and Jef Caers (Eds.)
- 237 **Petroleum Engineering** Moshood Sanni (Ed.)
- 238 **Geological Carbon Storage: Subsurface Seals and Caprock Integrity** Stephanie Vialle, Jonathan Ajo-Franklin, and J. William Carey (Eds.)
- 239 **Lithospheric Discontinuities** Huaiyu Yuan and Barbara Romanowicz (Eds.)
- 240 **Chemostratigraphy Across Major Chronological Eras** Alcides N. Sial, Claudio Gaucher, Muthuvairavasamy Ramkumar, and Valderez Pinto Ferreira (Eds.)
- 241 **Mathematical Geoenergy: Discovery, Depletion, and Renewal** Paul Pukite, Dennis Coyne, and Daniel Challou (Eds.)
- 242 **Ore Deposits: Origin, Exploration, and Exploitation** Sophie Decree and Laurence Robb (Eds.)
- 243 **Kuroshio Current: Physical, Biogeochemical and Ecosystem Dynamics** Takeyoshi Nagai, Hiroaki Saito, Koji Suzuki, and Motomitsu Takahashi (Eds.)
- 244 **Geomagnetically Induced Currents from the Sun to the Power Grid** Jennifer L. Gannon, Andrei Swidinsky, and Zhonghua Xu (Eds.)
- 245 **Shale: Subsurface Science and Engineering** Thomas Dewers, Jason Heath, and Marcelo Sánchez (Eds.)
- 246 **Submarine Landslides: Subaqueous Mass Transport Deposits From Outcrops to Seismic Profiles** Kei Ogata, Andrea Festa, and Gian Andrea Pini (Eds.)
- 247 **Iceland: Tectonics, Volcanics, and Glacial Features** Tamie J. Jovanelly
- 248 **Dayside Magnetosphere Interactions** Qiugang Zong, Philippe Escoubet, David Sibeck, Guan Le, and Hui Zhang (Eds.)
- 249 **Carbon in Earth's Interior** Craig E. Manning, Jung-Fu Lin, and Wendy L. Mao (Eds.)
- 250 **Nitrogen Overload: Environmental Degradation, Ramifications, and Economic Costs** Brian G. Katz
- 251 **Biogeochemical Cycles: Ecological Drivers and Environmental Impact** Katerina Dontsova, Zsuzsanna Balogh-Brunstad, and Gaël Le Roux (Eds.)
- 252 **Seismoelectric Exploration: Theory, Experiments, and Applications** Niels Grobbe, André Revil, Zhenya Zhu, and Evert Slob (Eds.)
- 253 **El Niño Southern Oscillation in a Changing Climate** Michael J. McPhaden, Agus Santoso, and Wenju Cai (Eds.)
- 254 **Dynamic Magma Evolution** Francesco Vetere (Ed.)
- 255 **Large Igneous Provinces: A Driver of Global Environmental and Biotic Changes** Richard E. Ernst, Alexander J. Dickson, and Andrey Bekker (Eds.)
- 256 **Coastal Ecosystems in Transition: A Comparative Analysis of the Northern Adriatic and Chesapeake Bay** Thomas C. Malone, Alenka Malej, and Jadran Faganeli (Eds.)
- 257 **Hydrogeology, Chemical Weathering, and Soil Formation** Allen Hunt, Markus Egli, and Boris Faybishenko (Eds.)
- 258 **At the Doorstep of Our Star: Solar Physics and Solar Wind** Nour E. Raouafi and Angelos Vourlidis (Eds.)
- 259 **Magnetospheres in the Solar System Remain Maggiolo** Nicolas André, Hiroshi Hasegawa, and Daniel T. Welling (Eds.)
- 260 **Ionosphere Dynamics and Applications** Chaosong Huang and Gang Lu (Eds.)
- 261 **Upper Atmosphere Dynamics and Energetics** Wenbin Wang and Yongliang Zhang (Eds.)
- 262 **Space Weather Effects and Applications** Anthea J. Coster, Philip J. Erickson, and Louis J. Lanzerotti (Eds.)
- 263 **Mantle Convection and Surface Expressions** Hauke Marquardt, Maxim Ballmer, Sanne Cottaar, and Jasper Konter (Eds.)
- 264 **Crustal Magmatic System Evolution: Anatomy, Architecture, and Physico-Chemical Processes** Matteo Masotta, Christoph Beier, and Silvio Mollo (Eds.)

Geophysical Monograph 265

---

**Global Drought and Flood**  
*Observation, Modeling, and Prediction*

Huan Wu  
Dennis P. Lettenmaier  
Qihong Tang  
Philip J. Ward

*Editors*

This Work is a co-publication of the American Geophysical Union and John Wiley and Sons, Inc.



**WILEY**

This edition first published 2021  
© 2021 American Geophysical Union

All rights reserved. No part of this publication may be reproduced, stored in a retrieval system, or transmitted, in any form or by any means, electronic, mechanical, photocopying, recording or otherwise, except as permitted by law. Advice on how to obtain permission to reuse material from this title is available at <http://www.wiley.com/go/permissions>.

### **Published under the aegis of the AGU Publications Committee**

---

Brooks Hanson, Executive Vice President, Science  
Carol Frost, Chair, Publications Committee  
For details about the American Geophysical Union visit us at [www.agu.org](http://www.agu.org).

The right of Huan Wu, Dennis P. Lettenmaier, Qihong Tang, and Philip J. Ward to be identified as the authors of the editorial material of this work has been asserted in accordance with law.

*Registered Office*  
John Wiley & Sons, Inc., 111 River Street, Hoboken, NJ 07030, USA

*Editorial Office*  
111 River Street, Hoboken, NJ 07030, USA

For details of our global editorial offices, customer services, and more information about Wiley products visit us at [www.wiley.com](http://www.wiley.com).

Wiley also publishes its books in a variety of electronic formats and by print-on-demand. Some content that appears in standard print versions of this book may not be available in other formats.

#### *Limit of Liability/Disclaimer of Warranty*

While the publisher and authors have used their best efforts in preparing this work, they make no representations or warranties with respect to the accuracy or completeness of the contents of this work and specifically disclaim all warranties, including without limitation any implied warranties of merchantability or fitness for a particular purpose. No warranty may be created or extended by sales representatives, written sales materials or promotional statements for this work. The fact that an organization, website, or product is referred to in this work as a citation and/or potential source of further information does not mean that the publisher and authors endorse the information or services the organization, website, or product may provide or recommendations it may make. This work is sold with the understanding that the publisher is not engaged in rendering professional services. The advice and strategies contained herein may not be suitable for your situation. You should consult with a specialist where appropriate. Further, readers should be aware that websites listed in this work may have changed or disappeared between when this work was written and when it is read. Neither the publisher nor authors shall be liable for any loss of profit or any other commercial damages, including but not limited to special, incidental, consequential, or other damages.

#### *Library of Congress Cataloging-in-Publication Data applied for*

Hardback ISBN 9781119427308

Cover Design: Wiley  
Cover Image: © Francesco Scatena/Shutterstock

Set in 10/12pt Times New Roman by Straive, Pondicherry, India

10 9 8 7 6 5 4 3 2 1

# CONTENTS

---

List of Contributors .....vii

Preface .....xiii

## Part I: Remote Sensing for Global Drought and Flood Observations

- 1 Progress, Challenges, and Opportunities in Remote Sensing of Drought**  
*Arash Modarresi Rad, Amir AghaKouchak, Mahdi Navari, and Mojtaba Sadegh* .....3
- 2 Remote Sensing of Evapotranspiration for Global Drought Monitoring**  
*Xiwu Zhan, Li Fang, Jifu Yin, Mitchell Schull, Jicheng Liu, Christopher Hain, Martha Anderson, William Kustas, and Satya Kalluri* .....29
- 3 Drought Monitoring Using Reservoir Data Collected via Satellite Remote Sensing**  
*Huilin Gao, Gang Zhao, Yao Li, and Shuai Zhang* .....47
- 4 Automatic Near-Real-Time Flood Mapping from Geostationary Low Earth Orbiting Satellite Observations**  
*Sanmei Li, Donglian Sun, Mitchell D. Goldberg, and Dan Lindsey* .....61
- 5 Global Flood Observation with Multiple Satellites: Applications in Rio Salado (Argentina) and the Eastern Nile Basin**  
*Beth Tellman, Jonathan A. Sullivan, and Colin S. Doyle* .....99
- 6 Integrating Earth Observation Data of Floods with Large-Scale Hydrodynamic Models**  
*Guy J.-P. Schumann and Jeffrey C. Neal* .....123

## Part II: Modeling and Prediction of Global Drought and Flood

- 7 Global Integrated Drought Monitoring with a Multivariate Framework**  
*Zengchao Hao* .....139
- 8 A Probabilistic Framework for Agricultural Drought Forecasting Using the Ensemble Data Assimilation and Bayesian Multivariate Modeling**  
*Mahkameh Zarekarizi, Hongxiang Yan, Ali Ahmadalipour, and Hamid Moradkhani* .....147
- 9 Integrating Soil Moisture Active/Passive Observations with Rainfall Data Using an Analytic Model for Drought Monitoring at the Continental Scale**  
*Feng Ma, Lifeng Luo, and Aizhong Ye* .....165
- 10 Global Flood Models**  
*Mark A. Trigg, Mark Bernhofen, David Marechal, Lorenzo Alfieri, Francesco Dottori, Jannis Hoch, Matt Horritt, Chris Sampson, Andy Smith, Dai Yamazaki, and Hongyi Li* .....181
- 11 Calibration of Global Flood Models: Progress, Challenges, and Opportunities**  
*Feyera A. Hirpa, Valerio Lorini, Simon J. Dadson, and Peter Salamon* .....201

<b>12 Digital Elevation Model and Drainage Network Data Sets for Global Flood and Drought Modeling</b> <i>Huan Wu, Jing Tao, Dai Yamazaki, Weitian Chen, Zequn Huang, Chaoqun Li, and John Kimball</i> .....	213
<b>13 Fundamental Data Set for Global Drought and Flood Modeling: Land Use and Land Cover</b> <i>Min Feng</i> .....	237
<b>Part III: Global Drought and Flood Risk Assessment, Management, and Socioeconomic Response</b>	
<b>14 Global River Flood Risk Under Climate Change</b> <i>Francesco Dottori, Lorenzo Alfieri, Lauro Rossi, Roberto Rudari, Philip J. Ward, and Fang Zhao</i> .....	253
<b>15 Direct Tangible Damage Classification and Exposure Analysis Using Satellite Images and Media Data</b> <i>Siquan Yang and Haixia He</i> .....	271
<b>16 Flood Risk and Monitoring Data for Preparedness and Response: From Availability to Use</b> <i>Andrew Kruczkiewicz, Mélody Braun, Shanna McClain, Helen Greatrex, Lacey Padilla, Laura Hoffman-Hernandez, Kara Siahaan, Miriam Nielsen, Brian Llamanzares, and Zachary Flamig</i> .....	289
<b>17 Global Flood Partnership</b> <i>Lorenzo Alfieri, Sagy Cohen, John Galantowicz, Guy J.-P. Schumann, Mark A. Trigg, Ervin Zsoter, Christel Prudhomme, Andrew Kruczkiewicz, Erin Coughlan de Perez, Zachary Flamig, Roberto Rudari, Huan Wu, Robert F. Adler, Robert G. Brakenridge, Albert Kettner, Albrecht Weerts, Patrick Matgen, Saiful A.K.M. Islam, Tom de Groeve, Francesco Dottori, and Peter Salamon</i> .....	307
<b>18 Drought and Flood Monitoring and Forecasting: Challenges and Opportunities Ahead</b> <i>Huan Wu, Dennis P. Lettenmaier, Qihong Tang, and Philip J. Ward</i> .....	323
<b>Index</b> .....	327



# LIST OF CONTRIBUTORS

---

**Robert F. Adler**

NASA Goddard Space Flight Center  
Greenbelt, Maryland, USA

**Amir AghaKouchak**

Department of Civil and Environmental Engineering,  
and Department of Earth System Science  
University of California Irvine  
Irvine, California, USA

**Ali Ahmadalipour**

Center for Complex Hydrosystems Research  
Department of Civil, Construction, and Environmental  
Engineering  
The University of Alabama  
Tuscaloosa, Alabama, USA

**Lorenzo Alfieri**

Disaster Risk Management Unit  
European Commission Joint Research Centre  
Ispra, Italy; *and*  
CIMA Research Foundation  
Savona, Italy

**Martha Anderson**

Agricultural Research Service  
United States Department of Agriculture  
Beltsville, Maryland, USA

**Mark Bernhofen**

School of Civil Engineering  
University of Leeds  
Leeds, United Kingdom

**Robert G. Brakenridge**

Institute of Arctic and Alpine Research  
University of Colorado  
Boulder, Colorado, USA

**Mélody Braun**

Red Cross Red Crescent Climate Centre  
The Hague, The Netherlands

**Weitian Chen**

Guangdong Province Key Laboratory for Climate  
Change and Natural Disaster Studies, and  
School of Atmospheric Sciences  
Sun Yat-sen University  
Guangdong, China

**Sagy Cohen**

Department of Geography  
The University of Alabama  
Tuscaloosa, Alabama, USA

**Simon J. Dadson**

School of Geography and the Environment  
Oxford University  
Oxford, United Kingdom

**Francesco Dottori**

Disaster Risk Management Unit  
European Commission Joint Research Centre  
Ispra, Italy

**Colin S. Doyle**

Cloud to Street  
New York, New York, USA; *and*  
Department of Geography and the Environment  
The University of Texas  
Austin, Texas, USA

**Li Fang**

NOAA NESDIS Center for Satellite Applications and  
Research  
College Park, Maryland, USA; *and*  
UMD-CISESS Cooperative Institute for Satellite Earth  
System Studies  
College Park, Maryland, USA

**Min Feng**

National Tibetan Plateau Data Center  
Institute of Tibetan Plateau Research  
Chinese Academy of Sciences  
Beijing, China; *and*  
University of Chinese Academy Sciences  
Beijing, China

**Zachary Flamig**

Center for Data Intensive Science  
University of Chicago  
Chicago, Illinois, USA

**John Galantowicz**

Atmospheric and Environmental Research Inc.  
Lexington, Massachusetts, USA

**Huilin Gao**

Zachry Department of Civil and Environmental Engineering  
Texas A&M University  
College Station, Texas, USA

**Mitchell D. Goldberg**

National Environmental Satellite, Data, and Information  
Service  
National Oceanic and Atmospheric Administration  
College Park, Maryland, USA

**Helen Greatrex**

International Research Institute for Climate and Society  
The Earth Institute, Columbia University,  
Palisades, New York, USA

**Tom de Groeve**

Disaster Risk Management Unit  
European Commission Joint Research Centre  
Ispra, Italy

**Christopher Hain**

NASA Marshall Space Flight Center  
Huntsville, Alabama, USA

**Zengchao Hao**

College of Water Sciences  
Beijing Normal University  
Beijing, China

**Haixia He**

National Disaster Reduction Center of China  
Ministry of Emergency Management of the People's  
Republic of China  
Beijing, China

**Feyera A. Hirpa**

School of Geography and the Environment  
Oxford University  
Oxford, United Kingdom

**Jannis Hoch**

Department of Physical Geography  
Utrecht University  
Utrecht, The Netherlands; *and*  
Deltares  
Delft, The Netherlands

**Laura Hoffman-Hernandez**

International Research Institute for Climate and Society  
The Earth Institute, Columbia University  
Palisades, New York, USA

**Matt Horritt**

School of Civil Engineering  
University of Leeds  
Leeds, United Kingdom

**Zequn Huang**

Guangdong Province Key Laboratory for Climate  
Change and Natural Disaster Studies, and  
School of Atmospheric Sciences  
Sun Yat-sen University  
Guangdong, China

**Saiful A.K.M. Islam**

Institute of Water and Flood Management  
Bangladesh University of Engineering  
and Technology  
Dhaka, Bangladesh

**Satya Kalluri**

Raytheon  
Upper Marlboro, Maryland, USA

**Albert Kettner**

Institute of Arctic and Alpine Research  
University of Colorado  
Boulder, Colorado, USA

**John Kimball**

Lawrence Berkeley National Laboratory  
Berkeley, California, USA; *and*  
University of Washington  
Seattle, Washington, USA

**Andrew Kruczkiewicz**

International Research Institute for Climate and Society  
The Earth Institute, Columbia University  
Palisades, New York, USA; *and*  
Red Cross Red Crescent Climate Centre  
The Hague, The Netherlands

**William Kustas**

Agricultural Research Service  
United States Department of Agriculture  
Beltsville, Maryland, USA

**Dennis P. Lettenmaier**

University of California, Los Angeles  
Los Angeles, California, USA

**Chaoqun Li**

Guangdong Province Key Laboratory for Climate Change and Natural Disaster Studies, and School of Atmospheric Sciences  
Sun Yat-sen University  
Guangdong, China

**Hongyi Li**

Department of Civil and Environmental Engineering  
University of Houston  
Houston, Texas, USA

**Sanmei Li**

Department of Geography and Geo-Information Science  
George Mason University  
Fairfax, Virginia, USA

**Yao Li**

Zachry Department of Civil and Environmental Engineering  
Texas A&M University  
College Station, Texas, USA

**Dan Lindsey**

National Environmental Satellite, Data, and Information Service  
National Oceanic and Atmospheric Administration  
Fort Collins, Colorado, USA

**Jicheng Liu**

NOAA NESDIS Center for Satellite Applications and Research  
College Park, Maryland, USA; *and*  
UMD-CISESS Cooperative Institute for Satellite Earth System Studies  
College Park, Maryland, USA

**Brian Llamanzares**

International Research Institute for Climate and Society  
The Earth Institute, Columbia University  
Palisades, New York, USA

**Valerio Lorini**

Disaster Risk Management Unit  
European Commission Joint Research Centre  
Ispra, Italy

**Lifeng Luo**

Department of Geography, Environment, and Spatial Sciences  
Michigan State University  
East Lansing, Michigan, USA

**Feng Ma**

School of Hydrology and Water Resources  
Nanjing University of Information Science and Technology  
Nanjing, China; *and*  
Department of Geography, Environment, and Spatial Sciences  
Michigan State University  
East Lansing, Michigan, USA

**David Marechal**

Guy Carpenter & Company GmbH  
Munich, Germany

**Patrick Matgen**

Luxembourg Institute of Science and Technology  
Esch-sur-Alzette, Luxembourg

**Shanna McClain**

Earth Sciences Division  
National Aeronautics and Space Administration  
Washington, DC, USA

**Hamid Moradkhani**

Center for Complex Hydrosystems Research  
Department of Civil, Construction, and Environmental Engineering  
The University of Alabama  
Tuscaloosa, Alabama, USA

**Mahdi Navari**

NASA Goddard Space Flight Center  
Greenbelt, Maryland, USA

**Jeffrey C. Neal**

School of Geographical Sciences  
University of Bristol  
Bristol, United Kingdom

**Miriam Nielsen**

International Research Institute for Climate and Society  
The Earth Institute, Columbia University  
Palisades, New York, USA

**Lace Padilla**

Department of Psychology  
Northwestern University  
Evanston, Illinois, USA

**Erin Coughlan de Perez**

International Research Institute for Climate and Society  
The Earth Institute, Columbia University  
Palisades, New York, USA; *and*  
Red Cross Red Crescent Climate Centre  
The Hague, The Netherlands; *and*  
Vrije Universiteit Amsterdam  
Amsterdam, The Netherlands

**Christel Prudhomme**

European Centre for Medium-range Weather Forecasts  
Reading, United Kingdom; *and*  
Centre for Ecology and Hydrology  
Wallingford, United Kingdom; *and*  
Department of Geography and Environment  
Loughborough University  
Loughborough, United Kingdom

**Arash Modarresi Rad**

Department of Computing  
Boise State University  
Boise, Idaho, USA

**Lauro Rossi**

CIMA Research Foundation  
Savona, Italy

**Roberto Rudari**

CIMA Research Foundation  
Savona, Italy

**Mojtaba Sadegh**

Department of Civil Engineering  
Boise State University  
Boise, Idaho, USA

**Peter Salamon**

Disaster Risk Management Unit  
European Commission Joint Research Centre  
Ispra, Italy

**Chris Sampson**

Fathom Global  
Bristol, United Kingdom

**Mitchell Schull**

NOAA NESDIS Center for Satellite Applications and  
Research  
College Park, Maryland, USA; *and*  
UMD-CISESS Cooperative Institute for Satellite Earth  
System Studies  
College Park, Maryland, USA

**Guy J.-P. Schumann**

School of Geographical Sciences  
University of Bristol  
Bristol, United Kingdom; *and*  
Institute of Arctic and Alpine Research  
University of Colorado  
Boulder, Colorado, USA

**Kara Siahhaan**

International Federation of Red Cross and Red  
Crescent Societies  
Geneva, Switzerland

**Andy Smith**

Fathom Global  
Bristol, United Kingdom

**Jonathan A. Sullivan**

School for Environment and Sustainability  
University of Michigan  
Ann Arbor, Michigan, USA

**Donglian Sun**

Department of Geography and Geo-Information  
Science  
George Mason University  
Fairfax, Virginia, USA

**Qihong Tang**

Institute of Geographic Sciences and Natural  
Resources Research  
Chinese Academy of Sciences  
Beijing, China

**Jing Tao**

Earth System Science Interdisciplinary Center  
University of Maryland  
College Park, Maryland, USA; *and*  
Lawrence Berkeley National Laboratory  
Berkeley, California, USA; *and*  
Department of Civil and Environmental Engineering  
University of Washington  
Seattle, Washington, USA

**Beth Tellman**

Cloud to Street  
New York, New York, USA; *and*  
The Earth Institute, Columbia University  
Palisades, New York, USA

**Mark A. Trigg**

School of Civil Engineering  
University of Leeds  
Leeds, United Kingdom

**Philip J. Ward**

Institute for Environmental Studies  
Vrije Universiteit Amsterdam  
Amsterdam, The Netherlands

**Albrecht Weerts**

Deltares  
Delft, The Netherlands; *and*  
Wageningen University and Research Centre  
Wageningen, The Netherlands

**Huan Wu**

School of Atmospheric Sciences  
Sun Yat-sen University  
Guangdong, China; *and*  
Southern Marine Science and Engineering Laboratory  
Guangdong, China; *and*  
Earth System Science Interdisciplinary Center  
University of Maryland  
College Park, Maryland, USA

**Dai Yamazaki**

Institute of Industrial Science  
The University of Tokyo  
Tokyo, Japan

**Hongxiang Yan**

Pacific Northwest National Laboratory  
U. S. Department of Energy  
Richland, Washington, USA

**Siquan Yang**

Division of Science and Informatization  
Ministry of Emergency Management of the People's  
Republic of China  
Beijing, China

**Aizhong Ye**

State Key Laboratory of Earth Surface and Ecological  
Resources  
Faculty of Geographical Science  
Beijing Normal University  
Beijing, China

**Jifu Yin**

NOAA NESDIS Center for Satellite Applications and  
Research  
College Park, Maryland, USA; *and*  
UMD-CISESS Cooperative Institute for Satellite Earth  
System Studies  
College Park, Maryland, USA

**Mahkameh Zarekarizi**

Center for Complex Hydrosystems Research  
Department of Civil, Construction, and  
Environmental Engineering  
The University of Alabama  
Tuscaloosa, Alabama, USA

**Xiwu Zhan**

NOAA NESDIS Center for Satellite Applications and  
Research  
College Park, Maryland, USA

**Shuai Zhang**

Department of Geological Sciences  
University of North Carolina at Chapel Hill  
Chapel Hill, North Carolina, USA

**Fang Zhao**

Key Laboratory of Geographic Information Science  
(Ministry of Education)  
School of Geographic Sciences  
East China Normal University  
Shanghai, China; *and*  
Potsdam Institute for Climate Impact Research  
Potsdam, Germany

**Gang Zhao**

Zachry Department of Civil and Environmental Engineering  
Texas A&M University  
College Station, Texas, USA

**Ervin Zsoter**

European Centre for Medium-range Weather Forecasts  
Reading, United Kingdom



# PREFACE

---

The increase in the frequency of drought and flood events due to changes in the global water and energy cycle poses higher risks to human settlements, especially those in floodplains and areas with frequent heat waves and deficit in precipitation, in an era of rapid population growth. Monitoring and forecasting of the occurrence, intensity, and evolution of drought and flood events are considered to be more and more important by humanitarian and government agencies for issuing timely warnings, monitoring ongoing hazards, and developing short-term and long-term risk assessments and management plans. In the past two decades, there have been significant advances in both numerical modeling and remote sensing approaches. These complementary approaches have been critical components in producing integrated information for droughts and floods.

This monograph reviews recent advances in the modeling and remote sensing of droughts and floods, covering many relevant topics including: (a) the currently available, widely used techniques and products for obtaining timely and accurate global-scale or continental-scale drought and flood information; (b) the features, strengths and weaknesses, and advances and challenges in each of these global products; (c) how these products have been used by humanitarian, government, and development sectors in recent natural disaster cases; and (d) discussions about the gaps between the products and end users, and insights for further improving the workflow in response activities from perspectives of both hazard information providers and users.

This book is organized into three closely connected sections. Part I focuses on remote sensing approaches for global drought and flood mapping. It starts with an overview of progress, challenges, and opportunities in remote sensing of drought. As critical components for drought monitoring, two well recognized remote-sensing-based products for evapotranspiration measurement and reservoir parameters (elevation, storage, and area) are then introduced and discussed in the following two chapters. Two widely used remote-sensing-based flood mapping products are described in the next two chapters, respectively, followed by a thoughtful chapter proposing an integration of Earth Observation (EO) data and numerical models, with the latter as the focus of the next section.

Part II summarizes current widely used modeling approaches and systems, including model physics, features,

validation, strength, limitations, and challenges in their further improvement and applications. In this section, the first three chapters are focused on modeling of drought using statistical, process-based or hybrid approaches. For flood modeling, an overview of the state-of-the-art flood models is presented in a dedicated chapter. An open challenge for almost all global flood models, i.e., large-scale calibration of models, is discussed in the following chapter. The rest of the section then focuses on two common data sets, i.e., derivations based on digital elevations model (DEM), and land use and land cover (LULC), which are fundamental for both drought and flood simulations.

Part III provides a review of recent advances in drought and flood damage estimation and risk assessment, and in-depth discussions on challenges in humanitarian response and management activities when integrating the hazard information from multiple products and data sources. Flood risk assessment under climate change is first introduced and discussed. Then practical activities in hazard response from national and international agencies are detailed in the next two chapters. The final chapter of this section describes the emerging role of the Global Flood Partnership (GFP), a network of scientists, users, and private and public organizations active in global flood response and risk management. The GFP shares flood information in near real-time for national environmental agencies and humanitarian organizations to support emergency operations and to reduce the overall socioeconomic impacts of disasters. A conclusion summarizes the whole book, with a brief discussion on existing challenges and the strategies of improving the monitoring and prediction of drought and flood.

Drought and floods have unsurprisingly become the hot topics of several recently published books. The uniqueness of this book, however, lies in the fact that: (a) it represents most of the ongoing modeling efforts, including current widely used products, and as chapter contributors are the developers of these products, this allows them to describe in detail and depth the strengths, weaknesses, advances and challenges in their further development and integration; (b) it brings together contributors from humanitarian, government, and development sectors, describing how these products are used in risk assessment and catastrophe response activities from a users' standpoint, shedding light on how to narrow the gap between product providers and users in both

expectation and communication. As a result, this book should appeal to a broad community of researchers, engineers, practitioners, policy makers, and decision makers, from various national and international agencies and non-governmental organizations (NGOs) working in drought and flood disaster management, and in sustainable and resilient construction. It should also be of interest to college students and teachers with interests in subjects including hydrology, remote sensing, meteorology, natural hazards, emergency management, and global change.

Last, we note that many of the chapters on floods are born out of presentations given at recent American Geophysical Union's Fall Meeting sessions on "Global Floods: Forecasting, Monitoring, Risk Assessment, and

Socioeconomic Response" and the annual meetings of the Global Flood Partnership (GFP). These sessions and meetings foster global flood forecasting, monitoring, and impact assessment efforts with the aim to strengthen preparedness and response and to reduce global flood losses.

**Huan Wu**

*Sun Yat-sen University, China*

**Dennis P. Lettenmaier**

*University of California, Los Angeles, USA*

**Qihong Tang**

*Chinese Academy of Sciences, China*

**Philip J. Ward**

*Vrije Universiteit Amsterdam, The Netherlands*



**Part I**

**Remote Sensing for Global  
Drought and Flood  
Observations**



# 1

## Progress, Challenges, and Opportunities in Remote Sensing of Drought

Arash Modarresi Rad<sup>1</sup>, Amir AghaKouchak<sup>2</sup>, Mahdi Navari<sup>3</sup>, and Mojtaba Sadegh<sup>4</sup>

### ABSTRACT

Drought, one of the most daunting natural hazards, is linked to other hazards such as heatwaves and wildfires, and is related to global and regional food security. Given the severe environmental and socioeconomic ramifications of droughts, comprehensive and timely analysis of droughts' onset, development, and recovery at proper spatial and temporal scales is of paramount importance. Droughts are categorized by different variables, such as precipitation, soil moisture, and streamflow, depending on the target of the analysis. The root cause of droughts, however, is sustained below-average precipitation. Large-scale oceanic and atmospheric circulations drive precipitation variability, and hence droughts should be analyzed from a continental to global perspective. Given the spatial scale of interest, as well as the poor spatial resolution and temporal inconsistency of ground observations, multisensor remotely sensed climatological, hydrological, and biophysical variables offer a unique opportunity to model droughts from different perspectives (meteorological, agricultural, hydrological, and socioeconomic) and at the global scale. It is also often required to model droughts using multiple indices and analyze feedbacks between droughts and other hazards, such as heatwaves. Multiple satellites, missions, and sensors offer invaluable information for multi-indicator modeling of droughts and their feedbacks with other natural hazards in an era of big data. Remote sensing satellite data, however, are associated with major challenges including temporal limitations, consistency within and between multiple sensors and data sets, reliability, lack of uncertainty assessment, managing data volumes, and paucity of research on translating remote sensing of drought into actionable science. With challenge comes opportunity. The focus of the scientific community should be on merging the information provided from different satellites and sensors, to underpin their uncertainties, and to offer long-term and consistent data sets for drought analysis.

### 1.1. INTRODUCTION

Drought is a recurring natural feature of climate and is defined as below-normal precipitation, usually over an extended period of time (Wilhite & Buchanan-Smith, 2005). Droughts cause billions of dollars of damage to multiple sectors globally, specifically to agriculture. Droughts may also cause, or co-occur with, other hazards such as heatwaves, which collectively escalate the ramifications of this natural hazard (Raei et al. 2018). Indeed, the concurrence of climatic extremes, in particular droughts and heat waves, can result in forest fires (Goulden, 2018; Silva et al., 2018; Taufik et al., 2017),

---

<sup>1</sup>Department of Computing, Boise State University, Boise, Idaho, USA

<sup>2</sup>Department of Civil and Environmental Engineering, and Department of Earth System Science, University of California Irvine, Irvine, California, USA

<sup>3</sup>NASA Goddard Space Flight Center, Greenbelt, Maryland, USA

<sup>4</sup>Department of Civil Engineering, Boise State University, Boise, Idaho, USA

land degradation and desertification (Hutchinson & Herrmann, 2016; Olagunju, 2015; Vicente-Serrano et al., 2015), water shortage for agriculture and urban water supply (AghaKouchak, Farahmand, et al., 2015; Gober et al., 2016; Khorshidi et al., 2019; Van Loon et al., 2016), and economic impacts, and may prompt water bankruptcy (Howitt et al., 2014; Madani et al., 2016). Therefore, the impacts of drought are complex and can propagate to regions outside the area of its occurrence. Drought is often categorized in four groups: meteorological, agricultural, hydrological, and socioeconomic (Dracup et al., 1980). Meteorological drought is defined as precipitation deficiency over a long period, and it best represents the onset of drought (Utah Division of Water Resources, 2007). An extended period of meteorological drought results in soil moisture deficit as evapotranspiration continues despite the lack of precipitation, which leads to agricultural drought (Cunha et al., 2015). Persistence of meteorological drought ultimately reduces overall water supply and drought is manifested in a hydrological form (Modaresi Rad et al., 2016). Socioeconomic drought then occurs as supply and demand of some economic goods are impacted by meteorological, agricultural, and hydrological droughts (Shiferaw et al., 2014). The observed changes in temporal patterns of precipitation associated with unsustainable water withdrawal may escalate the drought severity around the globe (Mallakpour et al., 2018; U.S. Global Change Research Program, 2018); and large-scale changes in weather patterns are likely to affect water storage around the globe and threaten water supply particularly in arid and semi-arid regions (Ault et al., 2014).

Drought detection requires observation of a plethora of different climatic and biophysical variables. Observations in situ, however, do not provide a uniform spatial distribution and are limited to populated areas, hence satellite-based observations provide a unique way to analyze and monitor drought at a global scale. Satellites offer observations for a wide range of climate variables such as precipitation, soil moisture, temperature, relative humidity, evapotranspiration, vegetation greenness, land-cover condition, and water storage (Aghakouchak, Farahmand, et al., 2015; R. G. Allen et al., 2007; L. Wang & Qu, 2009; Whitcraft et al., 2015). Although remote sensing provides more opportunities for the scientific community to monitor Earth systems and offer better understanding of drought impact at regional to global scales, it is not without flaws or challenges. The main challenge is the insufficient length of the observed records provided for the variables of interest. Other challenges include data consistency, ease of access, quantifying uncertainty, and development of appropriate drought indices, which will be discussed throughout this chapter.

## 1.2. PROGRESS IN REMOTE SENSING OF DRIVERS OF DROUGHT

This section presents the recent remote sensing techniques used for identification and quantification of drought as characterized by different climatic and biophysical variables.

### 1.2.1. Precipitation

A meteorological drought can be described as precipitation deficiency over a period of time (WMO, 1975), often represented in terms of an index of deviation from normal. Drought indices not only serve the scientific communities but they are also great tools for facilitating the decision-making and policy-making processes for stakeholders and managers when compared with the raw data. One of the most widely used and informative meteorological drought indices is the standardized precipitation index (SPI) developed by McKee et al. (1993). Several other meteorological drought indices have also been proposed, including, but not limited to, precipitation effectiveness (Thornthwaite, 1931), antecedent precipitation (API; McQuigg, 1954), rainfall anomaly (RAI; Van Rooy, 1965), drought area (Bhalme & Mooley, 1980), effective precipitation (Byun & Wilhite, 1999), and rainfall variability indices (Oguntunde et al., 2011). The SPI is currently being used in many national operational and research centers and was recognized as a global measure to characterize meteorological drought by the World Meteorological Organization (WMO, 2009). Computation of SPI requires measured rainfall data and a normalization process of monthly data, either by utilizing an appropriate probability distribution function (PDF) to transform the rainfall PDF (e.g., gamma or Pearson type III probability distribution) into a standard normal distribution (Khalili et al., 2011), or by utilizing a nonparametric approach (Hao & AghaKouchak, 2014). Precipitation deficit can be specified for different timescales (e.g., from 1 to 24 months) when using SPI, where precipitation abnormalities in shorter timescales reflect soil moisture wet/dry conditions and longer timescales portray the wet/dry conditions of subsequent processes such as streamflow, reservoir levels, and ultimately groundwater.

Since the root cause of droughts is deficit in precipitation, meteorological drought indices, and in particular SPI, are suitable indices for revealing the onset of drought (Hao & Aghakouchak, 2013). Indeed, precipitation is regarded as a key component in drought analysis. Clustering approaches have been used as a common practice to identify spatially homogeneous drought areas by utilizing meteorological drought indices such as SPI (Santos et al., 2010). Assessment of temporal variability of meteorological drought utilizing SPI, however, has shown formation of noncoherent clusters in spatiotemporal clustering (Modaresi Rad

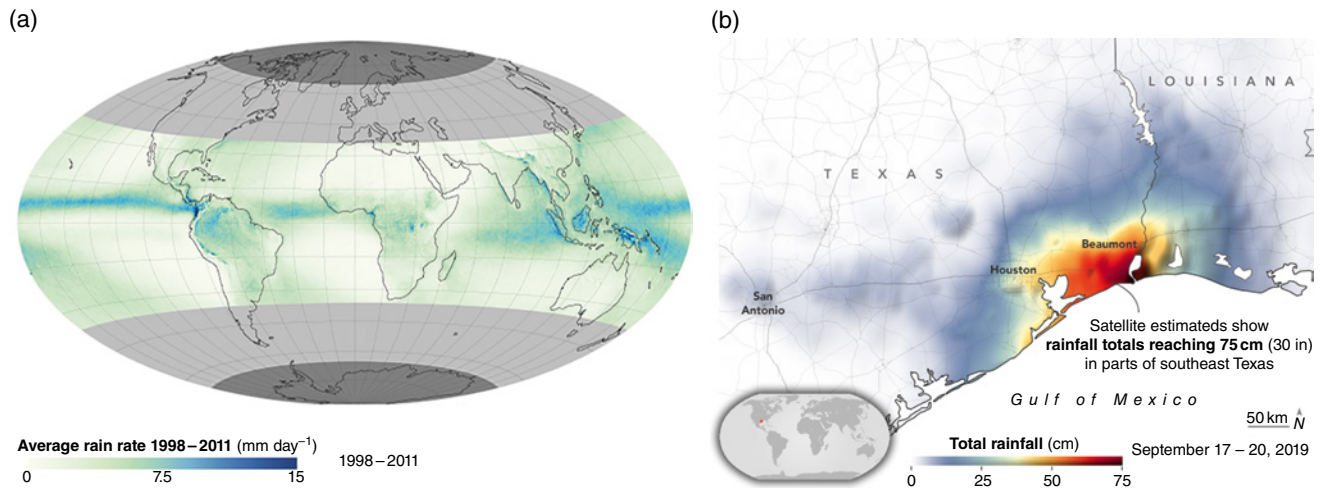


**Figure 1.1** Rainfall map by NASA's Tropical Rainfall Measuring Mission (TRMM) satellite. (a) Average rate of rainfall per day for the period of 1998-2011. (b) A tropical storm in southeast Texas causing record-breaking floods, produced using the IMERG precipitation product. (Courtesy: NASA's Earth observatory: <https://earthobservatory.nasa.gov/images>)

& Khalili, 2015). This is due to precipitation's large spatial variability, which creates diverse spatial patterns even at small scales. Considering spatial variability of precipitation is crucial, since a dense and evenly distributed network of gauging stations is required for describing spatiotemporal characteristics of drought. Similarly, ground-based weather radars also suffer from spatial discontinuity and are error prone due to contamination by surface backscatter, uncertainty of approximation of relation between reflectivity and rain rate, and bright band effects, making them unfeasible for global applications (Kidd et al., 2012; Wolff & Fisher, 2008). As a result, a more robust approach would be to use satellite observations that would produce gridded data as an input not only for drought models, but also for meteorological and hydrological models such as weather research and forecasting (WRF) and variable infiltration capacity (VIC).

Visible (VIS) satellite images provide information about cloud thickness and infrared (IR) images provide information on cloud top temperature and cloud height that are used to estimate precipitation rate via different retrieval algorithms (Joyce & Arkin, 1997; Sapiano & Arkin, 2009; Turk et al., 1999). Geostationary (GEO) VIS/IR satellites offer approximately a 15–30 min frequency of observations, but their accuracies are disputed. On the other hand, passive microwave (MW) sensors capture data of hydrometeor signals and scattering signals of raindrops, snow, and ice contents in the lower atmosphere and sense the bulk emission from liquid water, and therefore provide a more accurate estimation of precipitation rate (Behrangi et al., 2014). The MW sensors, however, often face difficulties distinguishing between light rain and clouds and have less frequent overpass (almost two observations per a

day). Therefore, it is suggested that a combination of both MW and VIS/IR satellite observations can result in more accurate estimations (Joyce et al., 2004). Currently, a variety of precipitation satellite data sets or products exist, amongst which that of the Tropical Rainfall Measuring Mission (TRMM) has found notable success towards improving the forecast of extreme events (Figure 1.1a). This data set is a joint mission between the National Aeronautics and Space Administration (NASA) and the Japan Aerospace Exploration Agency (JAXA) that advances the understanding of tropical rainfalls over the ocean by providing three-dimensional images. The mission was launched in 1997 and terminated in 2015, and the project was continued in 2014 by NASA's Goddard Space Flight Center and JAXA as Global Precipitation Measurement (GPM), with a new calibration standard for the rest of the satellite constellation and a core observatory that possessed a Dual-frequency Precipitation Radar (DPR) and a GPM Microwave Imager (GMI) (Hou et al., 2014). Other satellite precipitation data sets include the Climate Predicting Center (CPC) Morphing Technique (CMORPH; Joyce et al., 2004), CPC Merged Analysis of Precipitation (CMAP; Xie & Arkin, 1997), TRMM Multisatellite Precipitation Analysis (TMPA; Huffman et al., 2007), Special Sensor Microwave Imager (SSM/I; Ferraro, 1997), Global Precipitation Climatology Project (GPCP; Adler et al., 2003), Precipitation Estimation from Remotely Sensed Information using Artificial Neural Networks (PERSIANN; Figure 1.2; Ashouri et al., 2015; Hsu et al., 1997; S. Sorooshian et al., 2000), and the new GPM mission known as the Integrated Multisatellite Retrievals for GPM (IMERG; Figure 1.1b; Huffman et al., 2015).

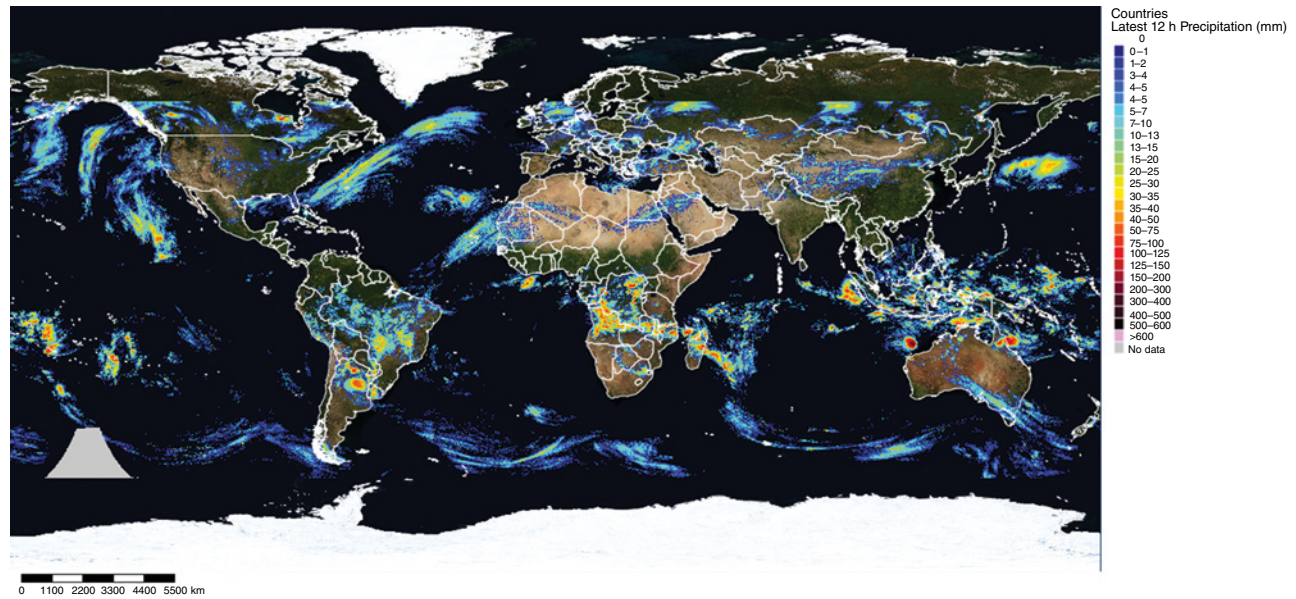


**Figure 1.2** Near real-time  $0.04^\circ$  precipitation information provided by the Global Water and Development Information (G-WADI) map server of University California at Irvine using the PERSIANN-Cloud Classification System (PERSIANN-CCS).

One of the major challenges associated with satellite precipitation data is measurement or inference uncertainty due to the presence of uncorrected biases (A. Sorooshian et al., 2008). Studies have shown that although TMPA can be used to produce reliable results when driving hydrological models for monthly streamflow simulation, it does not perform well at the daily time-scale (Meng et al., 2014). Since precipitation is a key variable in hydrology, the problem with uncertainty is further aggravated if it is left untreated in drought monitoring and hydrological modeling. As a result, several post-processing techniques have been developed for bias correction (Khajehi et al., 2018; Madadgar & Moradkhani, 2014). For further information regarding the validation process against ground-based measurements, interested reader is referred to AghaKouchak et al. (2012), Lu et al. (2018), Mateus et al. (2016), Nasrollahi et al. (2013), Y. Tian et al. (2009), and Xu et al. (2017). Another limitation of satellite precipitation data is associated with their short length of record. Drought analysis requires at least a minimum of 30 years of data (Mckee et al., 1993). Therefore, the near-real-time satellite precipitation products such as GPCP with nearly 19 years of recorded data cannot single-handedly be used to develop drought-monitoring systems. To remedy this shortcoming, near-real-time satellite data are combined with the long-term GPCP to produce the required timespan for drought calculation (AghaKouchak & Nakhjiri, 2012). In their study, AghaKouchak and Nakhjiri (2012) used a merged product of GPCP (1979–2009) and PERSIANN (2010 to the

present) in a Bayesian data-merging framework to produce a near-real-time meteorological drought monitoring system using SPI.

### 1.2.2. Soil Moisture

Agricultural drought is a result of precipitation deficit plus accumulated evapotranspiration over a prolonged period of time that eventually leads to extended periods of low soil moisture that affect crop yields and livestock production (Cunha et al., 2015). Agricultural drought disrupts the chain of supply and demand of agricultural products and contributes to socioeconomic drought (Wilhite & Glantz, 1985). Soil moisture is a key component of agricultural drought and defines the readily available water that plants can access from the soil through their root system. Soil moisture regulates the water and energy exchange between the land surface and the atmosphere. It also influences the partitioning of nonintercepted precipitation into surface runoff and infiltrations and influences the partitioning of net radiation into sensible, latent, and ground heat fluxes that are essential climate variables (WMO, 2006). Soil moisture condition directly reflects ecosystem functionality and agricultural productivity, therefore an agricultural drought influences the economy at local to global scales (IPCC, 2007; Ryu et al., 2014).

Warm surface temperature and rapidly decreasing soil moisture due to a lack of precipitation and hot temperatures are associated with rapidly developing drought conditions that are often known as “flash droughts” (M. C. Anderson et al., 2013; Otkin et al., 2016). Ford et al.

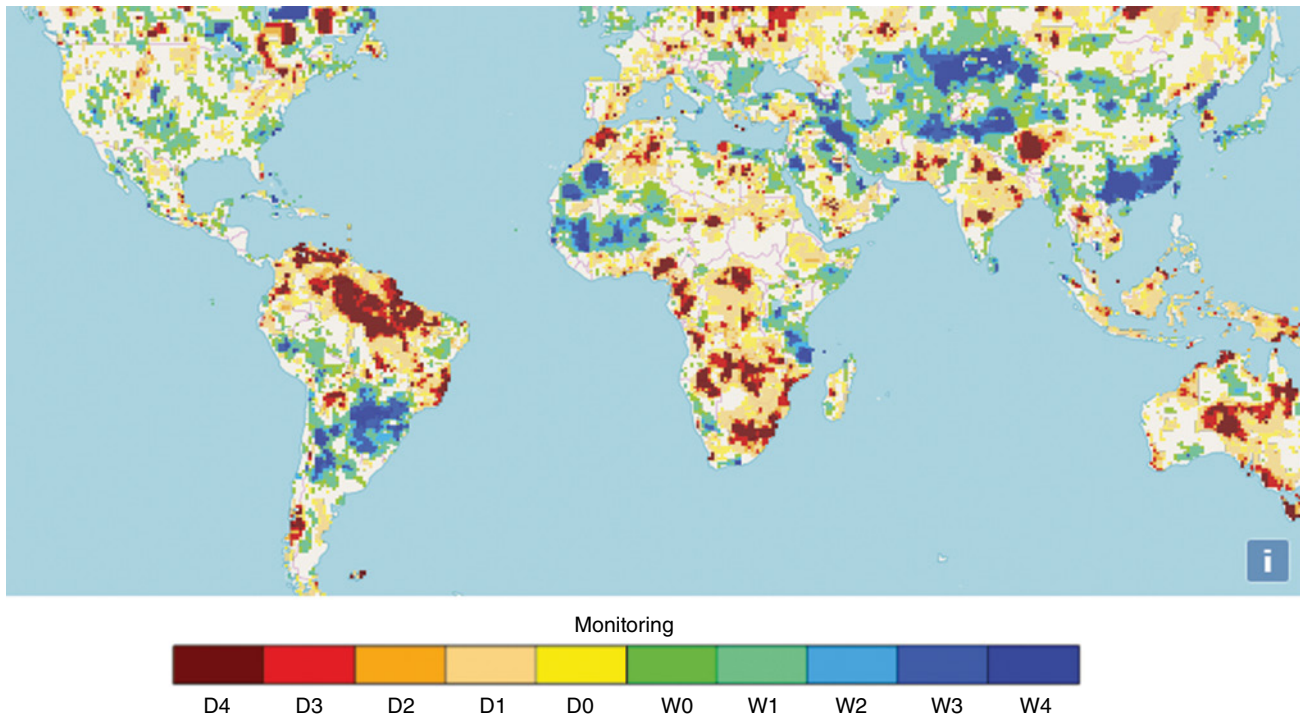


**Figure 1.3** Near real-time drought monitoring and prediction system by the Global Integrated Drought Monitoring and Prediction System (GIDMaPS) using the Standardized Soil Moisture Index (SSI) for February 2016 based on the Modern-Era Retrospective analysis for Research and Applications (MERRA) data set. D0 indicates abnormally dry; D1 moderate drought; D2 severe drought; D3 extreme drought; D4 exceptional drought; and the same applies to wetness (W) scale.

(2015) demonstrated that measurements of soil moisture in situ would drastically enhance the identification of flash droughts. Therefore, identification and quantification of drought at different timescales with high-resolution satellite imagery is crucial for decision making and developing drought mitigation strategies (D’Odorico et al., 2010). Several drought indices have been proposed to address deficiency in soil moisture, including the Crop Moisture Index (CMI; Palmer, 1965), Keetch–Byram Drought Index (KBDI; Keetch & Byram, 1968), Soil Moisture Percentile (Sheffield et al., 2004), Soil Moisture Deficit Index (SMDI; Narasimhan & Srinivasan, 2005), Scaled Drought Condition Index (SDCI) that uses multi-sensor data (Rhee et al., 2010), Microwave Integrated Drought Index (MIDI) that integrates precipitation, soil moisture, and land surface temperature derived from microwave sensors such as TRMM and AMSR-E (Zhang & Jia, 2013), Soil Moisture Drought Index (SODI; Sohrabi et al., 2015), and Standardized Soil Moisture Index (SSI; Hao & Aghakouchak, 2013; Figure 1.3).

What is required for agricultural drought and land surface models is the water content of the plant root zone in soil. This requires observatories in situ that are able to measure soil-water content at deeper layers of soil and provide more accurate estimations of soil moisture for purposes of drought monitoring as well as validation of

satellite estimations of soil moisture. The cosmic-ray soil moisture observing system (COSMOS; Zreda et al., 2012) and the German terrestrial environmental observatories (TERENO; Zacharias et al., 2011) are two examples of such in situ measurement networks. Moreover, the International Soil Moisture Network (ISMN) (<http://www.ipf.tuwien.ac.at/insitu>) provides a long record of global in situ soil moisture data, however, these measurements are typically available at point scales and contain significant spatial and temporal gaps. While point-based measurements are time consuming and costly, passive and active microwave sensor data retrieved from satellites readily provide spatiotemporally consistent observations of soil moisture from the top 5 cm of soil (Entekhabi et al., 2010; L. Wang & Qu, 2009). Given that agricultural drought monitoring requires information about soil moisture content of the entire soil column (i.e., surface and root zone), remotely sensed soil moisture data alone are not adequate for drought monitoring and complementary information about root zone soil moisture needs to be provided using modeling and data assimilation (e.g., Mladenova et al. 2019). Surface soil moisture data are derived mainly from passive or active microwave satellites (De Jeu et al., 2008; Njoku et al., 2003; Takada et al., 2009; Wagner et al., 1999). Currently, the Soil Moisture Active Passive (SMAP; Figure 1.4; Entekhabi et al., 2010) and

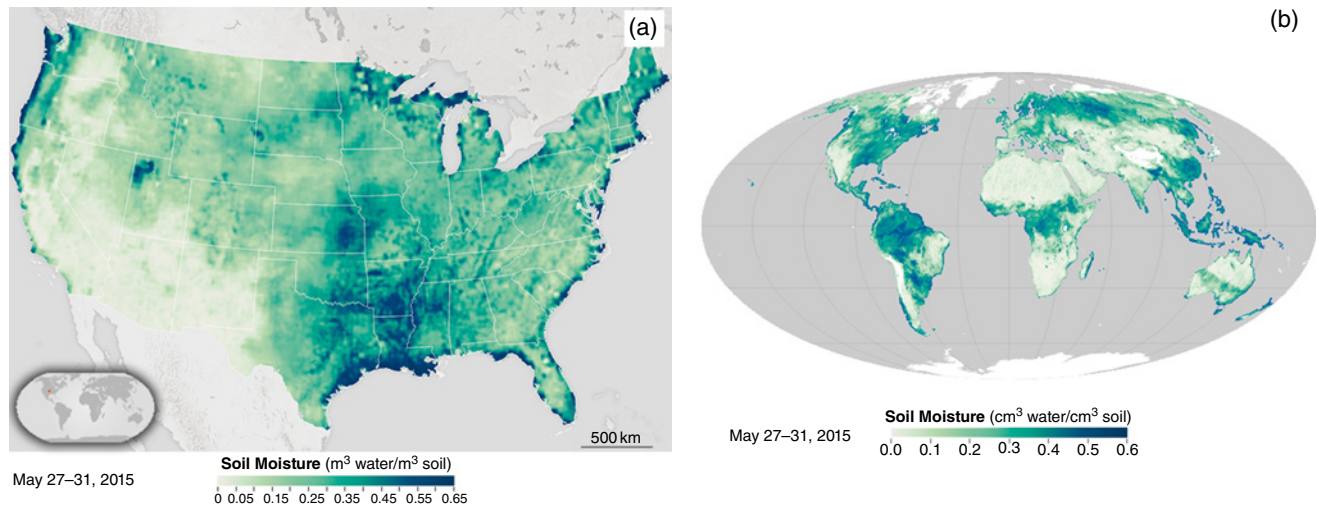


**Figure 1.4** Soil moisture observation by NASA's Soil Moisture Active Passive (SMAP) satellite. (a) Soil moisture observation of the United States. (b) Global view. (Courtesy of NASA's earth observatory: <https://earthobservatory.nasa.gov/images>).

the Soil Moisture Ocean Salinity (SMOS; Kerr et al., 2010) missions are the main sources of the remote-sensing-based soil moisture estimates. These data sets have been used extensively for drought monitoring (e.g., Mishra et al., 2017; Sadri et al., 2018; Sánchez et al., 2016). Soil moisture also can be inferred from other microwave sensors (Entekhabi et al., 2010; Martínez-Fernández et al., 2016; Moradkhani, 2008; Scaini et al., 2015) such as: the Scanning Multichannel Microwave Radiometer (SMMR), the SSM/I, the European Remote Sensing (ERS) scatterometer, the TRMM microwave imager, the Advanced Scatterometer (ASCAT), and Advanced Microwave Scanning Radiometer2 (AMSR2). Long-term soil moisture data appropriate for monitoring drought can be obtained through certain databases such as the Water Cycle Multimission Observation Strategy (WACMOS), which is derived from multiple satellites (Ambaw, 2013). Similarly, the European Space Agency's Climate Change Initiative (ESA CCI) offers a soil-moisture data set with a record of over 30 years that is particularly suitable for monitoring agricultural drought. The ESA CCI merges soil moisture retrievals of a number of different satellites and provides three types of product: active microwave, passive microwave, and combined active-passive microwave (Gruber et al., 2019). The ESA CCI soil-moisture data set, however, has large gaps over densely vegetated areas. Martínez-Fernández et al. (2016) show the reliability of the CCI soil-moisture data set for purposes of modeling agricultural drought.

Monitoring agricultural drought requires high-resolution data to reveal detailed variations of soil moisture. To improve the spatial resolution of soil moisture data, several downscaling methods have been used, such as

machine learning frameworks (Im et al., 2016; Park et al., 2017), DISaggregation based on Physical And Theoretical scale CHange (DISPATCH) which uses shortwave and thermal data from Moderate-Resolution Imaging Spectroradiometer (MODIS) to downscale SMOS data (Merlin et al., 2015), and Smoothing Filter-based Intensity Modulation (SFIM) which integrates microwave data from SMAP, Sentinel-1, and AMSR2 to downscale soil moisture data to an enhanced resolution of  $0.1^\circ \times 0.1^\circ$  (Santi et al. 2018).

### 1.2.3. Relative Humidity

Water vapor has a significant influence on Earth's climate and energy distribution as it displaces nearly half the trapped heat in an upward and poleward direction and is considered a natural greenhouse gas (Sherwood et al., 2010). Advances in remote sensing have made it possible to monitor water vapor and relative humidity through satellite sensors. Relative humidity is defined as the amount of water available in air with respect to the required water vapor for saturation at a specific temperature. Remotely sensed relative humidity data can be used as an early detection variable to monitor drought (Farahmand et al., 2015). A recently proposed Standardized Relative Humidity Index (SRHI) offers potential information about early drought detection and can be used in conjunction with other indices such as SPI or the Palmer Drought Severity Index (PDSI; Palmer, 1965) for drought monitoring and early warning systems (Farahmand et al., 2015; Figure 1.5). Studies also show that a combination of near-surface air temperature, vapor pressure deficit, and relative humidity can enhance



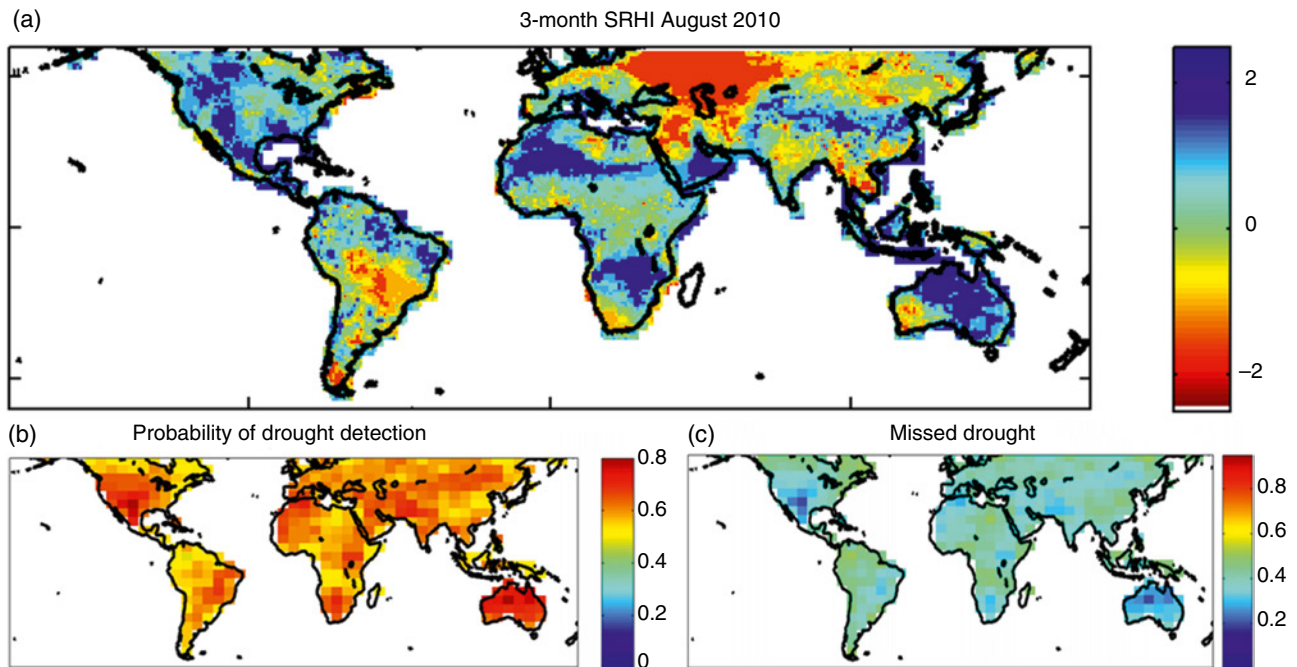


**Figure 1.5** Standardized Relative Humidity Index (SRHI) for (a) August 2010, (b) probability of drought detection, and (c) missed drought ratio, which indicates that relative humidity can be used in conjunction with other drought indices for early detection of drought onset (Farahmand et al., 2015).

the detection of drought onset (Behrangi et al., 2016). To detect onset of drought, Farahmand et al. (2015) used the Atmospheric Infrared Sounder (AIRS20) satellite's relative humidity data and developed a SRHI. The AIRS mission provides relative humidity data with a spatial resolution of  $1^\circ$  and covers a period ranging from 2002 to present. The authors suggested that due to the limited period of recorded data from AIRS for the purposes of drought analysis (< 30 years), the Gravity Recovery and Climate Experiment (GRACE) observations, Evaporative Stress Index data, and a combination of AIRS and reanalysis data sets could be used to extend the observation records.

Measurements of relative humidity via remote sensing are often undertaken with IR-based observing platforms (e.g., the AIRS20) (Fetzer et al., 2006; B. Tian et al., 2004). However, clouds tend to bias the IR observations, which is a major limiting factor since no observation of wet conditions will be available after a strict cloud screening (John et al., 2011). Another major issue is the variation of relative humidity due to changes in saturated vapor pressure, as it is significantly influenced by air temperature. Therefore, even with a fixed water vapor content, changes in air temperature will result in variations in relative humidity (Moradi et al., 2016). On the other hand, microwave sounder retrievals can produce large errors owing to modeling errors of Earth's limb radiances (e.g., Microwave Limb Sounder) (Lambert et al., 2007).

In general, too much uncertainty arises from observations of water vapor in diurnal and spatial distribution of the troposphere (Boyle & Klein, 2010), and having a coarse resolution of 2–3 km in both IR and microwave sounders, these instruments are unable to portray a detailed vertical structure of water vapor.

Vergados et al. (2015) used the Global Positioning System Radio Occultation (GPSRO) observations from the Constellation Observing System for Meteorology, Ionosphere, and Climate (COSMIC) mission that resolved the challenges associated with the presence of cloud. The authors demonstrated that the GPSRO-derived relative humidity data possess high quality. Sondeur Atmosphérique du Profil d'Humidité Intertropicale par Radiométrie (SAPHIR) from the Megha Tropiques satellite provides relative humidity data with temporal resolution of several observations per day and has six channels specifically for the water vapor absorption line at 183 GHz with a spatial resolution of 10 km at nadir for all the channels. Using the measurements of SAPHIR, Moradi et al. (2016) found larger diurnal amplitude over land compared to the ocean; larger oceanic amplitude over convective regions compared to subsidence regions; and showed that in tropical regions, relative humidity of the troposphere showed large inhomogeneity in diurnal variation. Brogniez et al. (2016) further improved the relative humidity estimates from the SAPHIR Sounder by producing uncertainty

estimates of the relative humidity through a Bayesian framework. Studies also suggested the appropriateness of using algorithms based on data from satellites such as the Advanced Very High Resolution Radiometer (AVHRR), National Oceanic and Atmospheric Administration (NOAA) Geostationary Operational Environmental Satellites (GOES), and MODIS to derive estimates of the surface level relative humidity (Han et al., 2005; Ramírez-Beltrán et al., 2019).

The frequency of unusually dry and hot conditions has increased in various parts of the world (Griffin & Anchukaitis, 2014; Seager & Hoerling, 2014). Some studies reported that the ever-increasing anthropogenic radiative forcing is responsible for the recent changes in Earth's hydrological cycle (Chikamoto et al., 2017; Littell et al., 2016; Williams et al., 2015). Chikamoto et al. (2017) demonstrated that droughts enhance wildfire probabilities in forested systems that take a huge toll on the economy, environment, and local communities in the countryside. Wildfire smoke tremendously increases the level of air pollution and therefore proliferates mortality, and respiratory and cardiovascular morbidity. Accurate measurement of relative humidity is essential for retrieving Aerosol Optical Thickness (AOT) and quantifying particulate matter (PM). Aerosol optical thickness can be derived from the MODIS on board NASA's Terra and Aqua satellites. The humid air surrounding hygroscopic aerosols causes swelling and this will substantially increase the scattering efficiency of the particles (Hess et al., 1998; Twohy et al., 2009). Gupta et al. (2006) found that a relative humidity ranging from 50% to 80% would increase AOT less than 5%, whereas a relative humidity range of 98–99% results in a more pronounced increase (more than 25%). These results indicate that relative humidity data can be used to enhance the measurements of PM and devise mitigation strategies (Bowman & Johnston, 2005) to reduce the adverse impacts of the hazard (i.e., drought-associated events such as wildfires).

#### 1.2.4. Evapotranspiration

Evapotranspiration (ET) is an important variable in agriculture, accurate estimation of which is essential for modeling agricultural drought. Evapotranspiration directly affects socioeconomic systems and agriculture, as irrigation water demand and crop yield are determined by this variable. Ecosystem and agriculture responses to drought are depicted by the ratio between actual ET (AET) and potential ET (PET) (Thornthwaite, 1948). Accordingly, several drought indices have been proposed that incorporate ET into their calculation including the PDSI, Crop Water Stress Index (CWSI; Jackson et al., 1981), Supply–Demand Drought Index (SDDI; Rind et al., 1990), Water Deficit Index (WDI; Moran

et al., 1994), Reconnaissance Drought Index (RDI; Tsakiris & Vangelis, 2005), Evaporative Drought Index (EDI; Yao et al., 2010), Standardized Precipitation Evapotranspiration Index (SPEI; Vicente-Serrano et al., 2010), Evaporative Stress Index (ESI; M. C. Anderson et al., 2016), Drought Severity Index (DSI; Mu et al., 2013), Green Water Scarcity Index (GWSI; Núñez et al., 2013), Green Water Stress Index (GrWSI; Wada, 2013), Standardized Palmer Drought Index (SPDI; Ma et al., 2014), Multivariate Drought Index (MDI; Rajsekhar et al., 2015), effective Reconnaissance Drought Index (eRDI; Tigkas et al., 2017), Normalized Ecosystem Drought Index (NEDI; Chang et al., 2018), and Aggregate Drought Index (ADI; S. Wang et al., 2018).

Both RDI and SPEI are widely used water-balance-system agricultural drought indices that utilize precipitation and PET as their input (Tsakiris et al., 2007; Vicente-Serrano et al., 2010). While SPEI uses the Penman–Monteith method to derive PET (Figure 1.6), RDI utilizes temperature-based methods to estimate PET and can use satellite-retrieved air temperature data (Dalezios et al., 2012). Recently, Tigkas et al. (2017) modified the RDI index by substituting precipitation by effective precipitation (the amount of water that contributes to crop development and is absorbed by the root system), which can more effectively describe plant water consumption. The modified index (eRDI) has the advantage of considering different stages of crop development and has shown higher correlation to reduction of crop yield in the location studied (Tigkas et al., 2017). Despite the advantages of utilizing the temperature-based method of PET, it suffers from several shortcomings as other factors such as net radiation, wind speed, and relative humidity that have strong influence on PET are being neglected in the process (Donohue et al., 2010; McVicar et al., 2012). Ma et al. (2014) outlined some issues regarding the climatic water balance system used by SPEI and suggested that SPEI would be more realistic if soil-moisture-related hydrometeorological processes are considered. They redefined the procedure of PDSI calculation on the basis of the mathematical framework of SPEI and proposed a new multiscalar drought index. While indices such as SPI or PDSI can be used as early warning systems to detect potential drought imposed on an ecosystem, NEDI offers an actual drought stress response to limited water availability.

The remotely sensed methods of ET estimation can be categorized into four groups, including water balance systems (R. G. Allen et al., 1998; Senay, 2008), surface energy balance systems (R. G. Allen et al., 2007; Anderson & Kustas, 2008), vegetation indices (Glenn et al., 2011), and hybrid approaches that incorporate vegetation indices and surface temperature measurements (Kalma et al., 2008; Yang & Shang, 2013). MODIS data have

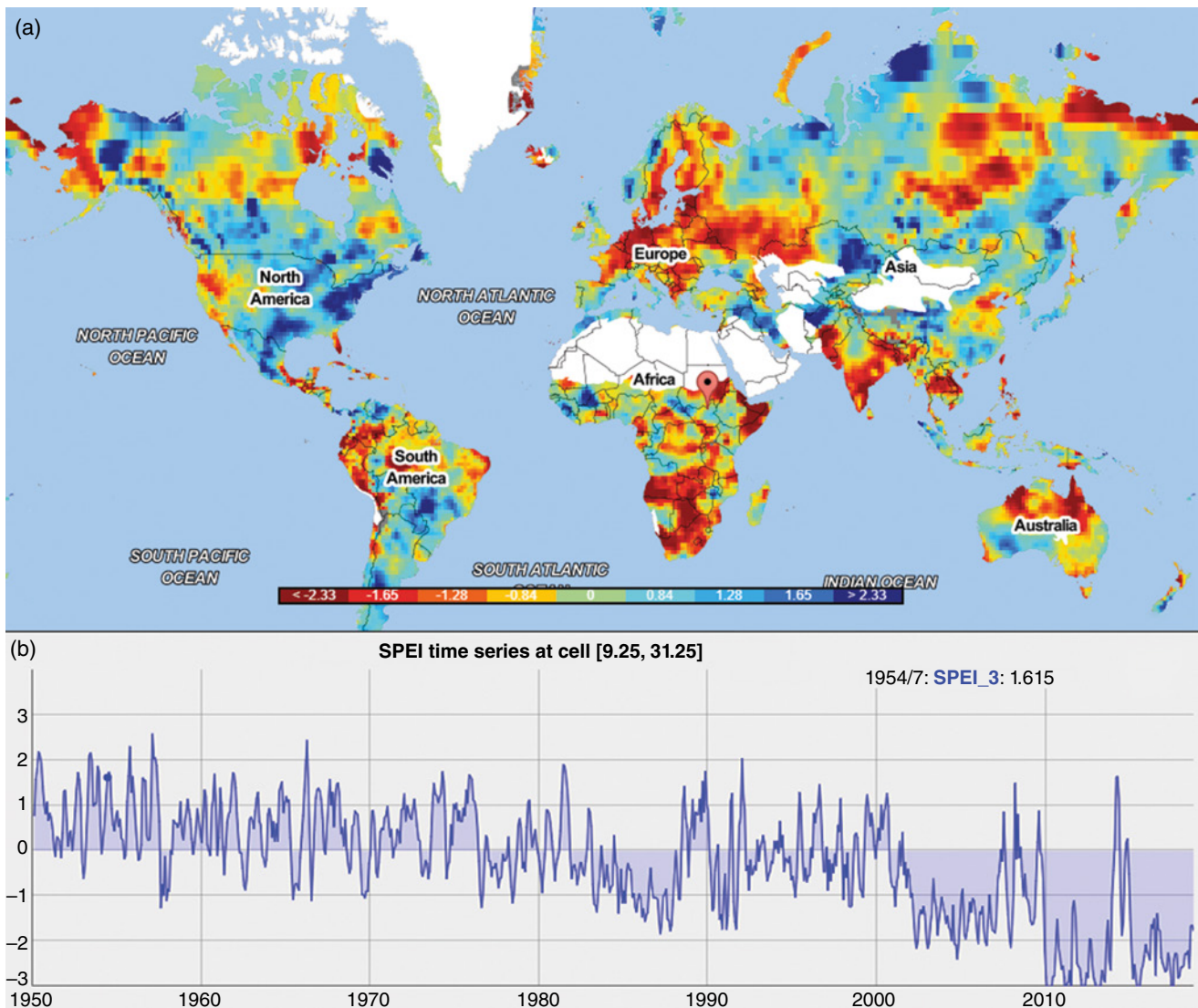


**Figure 1.6** Three-month Standardized Precipitation Evapotranspiration Index (SPEI) with  $1^\circ$  spatial resolution. (a) Global view of SPEI for November 2018. (b) Time series of SPEI for  $9.25^\circ$  E and  $31.25^\circ$  S in Africa. (Source: The Standardized Precipitation Evapotranspiration Index (SPEI), <http://spei.csic.es/map/maps.html>)

been frequently used worldwide to obtain land surface temperature data and derive ET for purposes of drought monitoring such as estimation of Evaporative Stress Index (ESI; Figure 1.7; M. C. Anderson et al., 2007) and DSI. Some other satellites capable of measuring land surface temperature include Advanced Spaceborne Thermal Emission and Reflection Radiometer (ASTER) on board Terra, Landsat, AVHRR on board polar orbiting platforms of NOAA, and visible and infrared imager (MVIRI) on board Meteosat satellites. The ECOSystem Spaceborne Thermal Radiometer Experiment on Space Station (ECOSTRESS) is a multiple wavelength imaging spectrometer that was launched on 29 June 2018 to the International Space Station (ISS) that provides ET

estimates. This product has a spatial resolution of  $\sim 70$  m and temporal resolution of approximately 3 days and is variable depending on ISS. Different ECOSTRESS data products are available for download through the United States Geological Survey (USGS) satellite image query tool (<https://earthexplorer.usgs.gov/>).

### 1.2.5. Snow

Snow and ice are key components of the hydrological cycle. The lack of snow and ice storage in the snow-dominated regions significantly impacts the availability of water throughout the dry seasons, and influences reservoir operation, flood risk management, recreation,

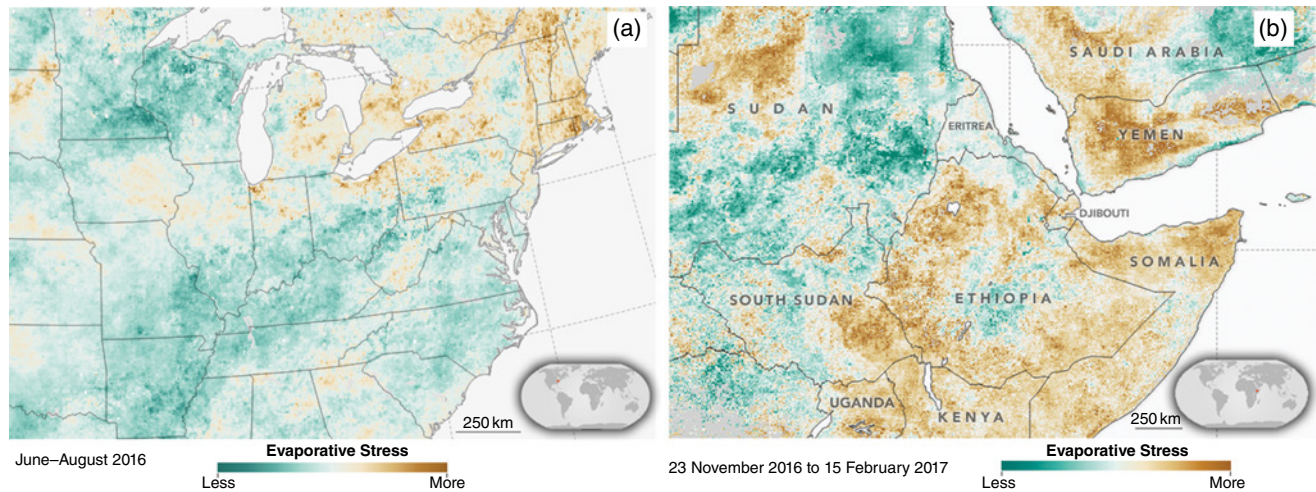


**Figure 1.7** Evaporative Stress Index (ESI) derived from observations of land surface temperatures and leaf area index from the Moderate Resolution Imaging Spectroradiometer (MODIS) on NASA's Terra and Aqua satellites and the Visible Infrared Imaging Radiometer Suite (VIIRS) of the Suomi National Polar-orbiting Partnership (NPP). (a) The drought in New England that put crops and businesses under stress. (b) The drought that reduced food production and increased famine in the Greater Horn of Africa. (Courtesy: NASA's earth observatory: <https://earthobservatory.nasa.gov/images>)

tourism, energy production, navigation, and river ecology (Staudinger et al., 2014). Therefore, snow shortage in snow-dominated mountain watersheds drives a range of adverse economic and social outcomes. Studies suggest that the occurrence of earlier peak discharge in western United States due to a warmer climate results in increased periods of summer water stress, which can in turn change forest structure (Harpold et al., 2014; Harpold, 2016). The continuous changes in the climate of snow-dominated watersheds (i.e., less snow, more rain, and earlier snowmelt) motivated researchers to introduce the concept of snow drought (Hatchett & McEvoy, 2018). Only a little research has been undertaken, however, with respect to developing a snow-based indicator of drought. Currently, there is no generally accepted classification scheme for snow droughts. Three key metrics, the peak snow water equivalent (SWE), the date of peak SWE (DPS), and the snow disappearance date (SDD), however, have been used to characterize snow drought in the mountainous watersheds. The concept of snow drought can be defined as below-average SWE at approximately when the maximum SWE typically occurs (Hatchett & McEvoy, 2018). Different definitions of snow drought have been proposed throughout the literature, including Van Loon and Van Lanen (2012) and Harpold et al. (2017).

Van Loon and Van Lanen (2012) described different scenarios of snow related drought according to their development: (a) rain-to-snow season drought, (b) cold snow season drought, and (c) warm snow season drought. Rain-to-snow season drought is developed due to a shortage of rainfall in the rain season (spring, summer and/or

autumn) and ends in snow season (winter) with precipitation being in the form of snow. Consequently, soil moisture, streamflow, and groundwater remain relatively low until the upcoming melt season. Cold snow season drought is a result of abnormally low temperature in the snow season and a possible coincidence with below-average precipitation that can be categorized into three subtypes of A, B, and C. Subtype A describes climates with continuous snow cover during winter and below zero temperature. Early beginning of the snow season is the main driver of this drought type. Subtype B has the same climate as A, however, delay in snowmelt due to low temperature at the end of winter drives this type of snow drought. Subtype C is climate with a temperature around zero and limited snow accumulation in winter. Snowmelt often provides recharge to groundwater and streamflow during snow season. An abnormal temperature drop in winter results in an intermediate shortage of water for a few weeks to months duration.

Harpold et al. (2017) divided snow drought into two categories: (a) warm snow drought, where accumulated precipitation during October–March is larger than the long-term average and SWE on 1st April is less than the long-term average; (b) dry snow drought, where accumulated precipitation for the same period is less than the long-term average and SWE on 1st April is less than the long-term average SWE.

In addition to the conceptual definition of snow drought, operational systems require relevant indicators to monitor snow drought. These indicators should provide insight on frequency, severity, and duration of snow

drought and help to develop prevention and mitigation strategies (Paneque, 2015). Indices such as SPI or PDSI are widely used to characterize hydrological droughts, however, these indices do not explicitly account for the effects of snow on water availability in snow-dominated watersheds (Mote et al., 2016). Staudinger et al. (2014) proposed a drought index that would account for snow. This new index, termed Standardized Snow Melt and Rain Index (SMRI), is calculated similar to the SPI but uses summation of snowmelt and rain as input. The authors proposed an algorithm based on temperature threshold that does not require snow data and utilizes temperature and precipitation to model snow. It should be noted that the output of any snow model could be used to calculate the index. Knowles et al. (2017) developed a snow aridity index (SAI) to assess ecosystem disturbance based on a long history of snow remote sensing. The SAI is defined as a ratio of the sum of 1st April to 31st August PET to maximum SWE ( $PET/SWE$ ; Figure 1.8). It can be argued that SAI is a suitable index for characterizing snow drought since it uses both potential evapotranspiration and SWE (Knowles et al., 2017, 2018).

Snowpack is often characterized in terms of snow albedo (SA), snow depth (SD), SWE, DPS, snow covered area (SCA), and fractional snow-covered area (fSCA) (Kongoli et al., 2012). Remote sensing can effectively describe the relationship between snowpack dynamics and climate variability (Guan et al., 2012). Using remote sensing techniques and retrieval algorithms to measure snow-related variables may provide insight for real-time snow drought monitoring. The following provides a very

short review of different remote sensing data and products that can be used to characterize snowpack.

Snow possesses a strong spectral gradient that ranges from high albedo in visible wavelengths to low reflectance in middle infrared wavelengths. Therefore, a commonly used method such as the band ratios can be utilized to map and monitor snow cover (Lettenmaier et al., 2015). The Normalized Difference Snow Index (NDSI) is one that shows the presence of snow on the ground. The NDSI algorithm distinguishes between snow and most cloud types, therefore, it better characterizes the snow cover areas than fSCA. The NDSI utilizes the reflectance ratios to detect snow and is described as the normalized difference between green and SWIR reflectance ( $(R_{Green} - R_{SWIR2}) / (R_{Green} + R_{SWIR2})$ ) (Hall et al., 2002). Hatchett and McEvoy (2018) suggested using NDSI in conjunction with data from ground-based observation networks to monitor snow drought. In forested regions, however, the NDSI has shown poor snow identification accuracy and the recently developed Normalized Difference Forest Snow Index (NDFSIS) can produce higher identification accuracy. The NDFSIS utilizes near-infrared in place of the green band, which has a higher reflectance that is useful when there is snow in a forested area (X. Y. Wang et al., 2015).

Several satellites are capable of detecting fSCA, such as the AVHRR, MODIS, and Landsat. However, a common issue with AVHRR is the inadequacy of its 1 km spatial resolution for snow mapping on small catchments (Simpson et al., 1998; H. Xu et al., 1993). Rott et al. (2010) suggested that the Cold Regions Hydrology High-Resolution Observatory (CoReH2O) from the ESA

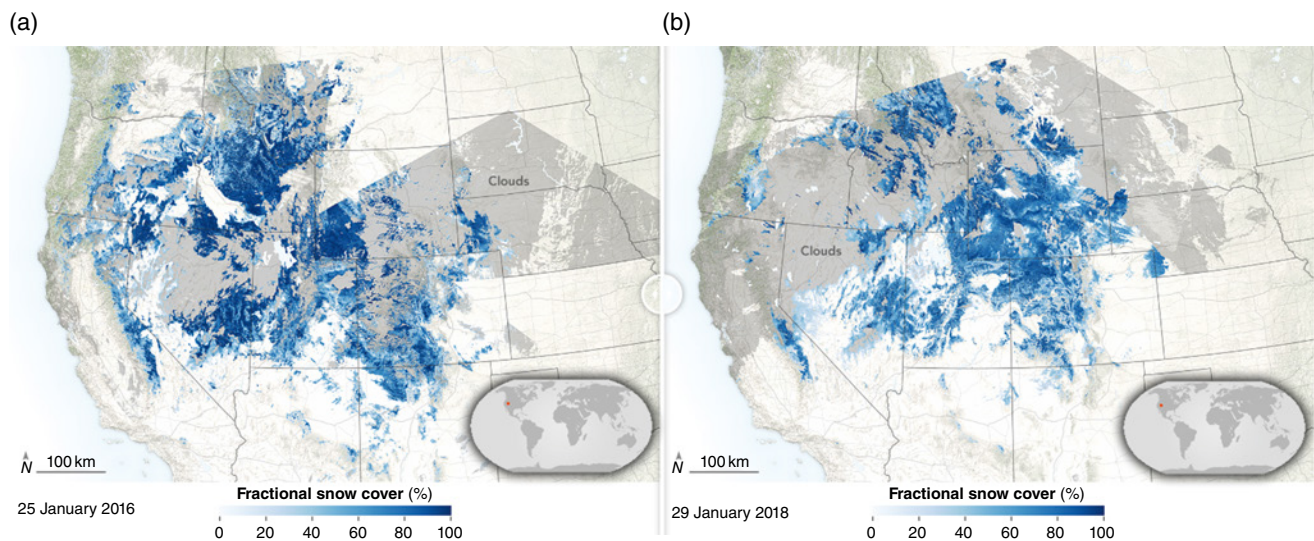


**Figure 1.8** A below-normal snowpack observed by the Moderate Resolution Imaging Spectroradiometer (MODIS) on NASA's Terra satellite. (a) Percent of fractional snow cover on 25 January 2016. (b) Below normal conditions in 29 January 2018. (Courtesy of NASA's earth observatory: <https://earthobservatory.nasa.gov/images>)

would deliver accurate and spatially detailed observations of snow mass. MODIS and Landsat Thematic Mapper (TM) alleviate this shortcoming to some extent by offering observations with a spatial resolution of 250 m and 30 m, respectively (Hall et al., 2002). A major concern regarding the optical-based satellites, however, is the discontinuity of observations due to the presence of clouds. Clouds hinder the spatiotemporal consistency of snow cover due to having similar reflectance properties to snow in a wide range of the electromagnetic spectrum (Aghakouchak, Farahmand, et al., 2015). On the other hand, microwave measurements can be used to estimate fSCA and SD even in the presence of clouds, since they do not depend on sunlight reflection. Similar to optical-based satellites, the microwave observations become flawed once SD exceeds 30 cm and in melting conditions (Foster et al., 1997; Walker & Goodison, 1993). Therefore, more accurate and consistent measurements of SD retrievals can be achieved through an integrated framework by combining observations from both types of satellites (Durand et al., 2008; Foster et al., 2011). In an effort to simulate the spatiotemporal distribution of SWE in mountainous regions, the NASA Jet Propulsion Laboratory (JPL) Airborne Snow Observatory (ASO) provides near-weekly lidar surveys. The derived SDs obtained from lidar scanners are then assimilated into hydrological models to produce higher temporal resolution of SWE distribution and volume. Recently, Hedrick et al. (2018) combined the iSnobal physically based distributed snowmelt model with ASO and produced daily SWE images with spatial resolution of 50 m.

Snow water equivalent is a critical parameter for hydrological applications and the characterization of snowpacks, and is commonly estimated using passive microwave signals utilizing empirical relationships or radiative transfer models. Well-known limitations of spaceborne passive microwave data, such as coarse spatial resolution, saturation in deep snowpack, and signal loss in wet snow, however, present major drawbacks for passive microwave retrieval algorithms. Brodzik et al. (2016) developed high-resolution passive microwave brightness temperature data that can be used to improve the SWE estimate in mountainous regions with complex physiography.

Peak SWE is an important variable in snow hydrology, traditionally, 1st April has been set as the date of peak SWE, however, many studies have shown that the peak SWE happens at different times. Margulis et al. (2016) showed that the assumption of 1st April peak SWE can lead to a significant underestimation of peak SWE. They also highlighted the role of elevation and interannual variability of peak SWE in the Sierra Nevada (California). Snow models and observations in situ are complementary tools that can be used in conjunction with remote

sensing to accurately estimate the peak SWE and the date of peak SWE.

Although application of snow-based drought indices for drought monitoring by remote sensing has been increased recently (Knowles et al., 2017; Sadegh, Love, et al., 2017; Staudinger et al., 2014), the majority of research incorporates satellite observations of snow data into land-surface and climate models (He et al., 2011; Kumar et al. 2014, Margulis et al., 2006, 2016). Global drought models based on snow are primarily challenged by the time lag between occurrences of precipitation as snow and changes in ground and surface waters that could vary between weeks to months depending on catchment characteristics and climate (Aghakouchak, Farahmand, et al., 2015; Van Loon & Van Lanen, 2012). As a final note, interested readers are encouraged to explore the different snow drought tools available online at (<https://www.drought.gov/drought/data-maps-tools/snow-drought>).

### 1.2.6. Groundwater

Prolonged meteorological droughts can severely affect groundwater levels and the problem is further exacerbated if it is followed by an anthropogenic drought (Aghakouchak, Feldman, et al., 2015; Alborzi et al. 2018). A decrease in groundwater recharge results in lower groundwater discharge and storage, a condition that is defined as a groundwater drought (Mishra & Singh, 2010). The lack of any imposed restriction for groundwater abstraction enhances hydrological drought, which is often overlooked due to poor understanding of hydrological cycle relations (Van Loon et al., 2016). The overuse of groundwater due to anthropogenic influences not only magnifies the drought condition, but also can cause permanent damage such as decreases in groundwater storage capacity and subsequent land subsidence (Famiglietti et al., 2011; Faunt et al., 2015; Taravatroy et al. 2018). The lack of continuous spatiotemporal measurements of groundwater levels at a groundwater monitoring station (well) makes it difficult to characterize groundwater drought; however, with the launch of the GRACE satellites it has become possible to study the dynamics of water storages at a global scale (Wahr et al., 2006). The GRACE (2002–2017) and GRACE Follow-On (2018 to present) satellites monitor changes in water storage comprising groundwater, surface water reservoir, soil moisture, and snow water storage components.

The GRACE missions provide global changes in total water storage by converting gravity anomalies into changes of water equivalent height (Rodell & Famiglietti, 2002; Figure 1.9). The observed terrestrial water storage (TWS) from GRACE has spatial resolution of 150,000 km<sup>2</sup> per grid that cannot be used for regional assessments;